



Two Methods for Determination of Transport Numbers in Ion-Exchange Membranes

C. Tian¹ · K. R. Kristiansen² · S. Kjelstrup² · V. M. Barragán¹ 

Received: 22 September 2021 / Accepted: 25 October 2021 / Published online: 9 November 2021
© The Author(s), under exclusive licence to Springer Science+Business Media, LLC, part of Springer Nature 2021

Abstract

Chronopotentiometry and electromotive force methods were used to determine ion transport numbers in two homogeneous and highly selective cation- and anion-exchange membranes. NaCl aqueous solutions of different concentrations, varying from $1 \text{ mol}\cdot\text{m}^{-3}$ to $100 \text{ mol}\cdot\text{m}^{-3}$ were used to analyze the possible impact of the electrolyte concentration on the results obtained by both methods. Cation transport numbers close to unity for the cation exchange membrane and to zero for the anion-exchange membrane were found for both membrane types with both methods when the NaCl-concentration exceeded $10 \text{ mol}\cdot\text{m}^{-3}$. At the lowest concentrations, a systematic deviation from ideal behavior was seen, mainly in the electromotive force method, possibly due to a higher contribution from transport of water. The cation transport number estimated by the electromotive force method was systematically lower than the number obtained from chronopotentiometry, probably due to larger concentration polarization at low electrolyte concentration. We conclude that chronopotentiometry is a relatively rapid and precise technique for ion transport number determination at electrolyte concentrations for which membranes maintain a good selectivity for the measurement conditions used.

Keywords Chronopotentiometry · Electromotive force · Ion-exchange membrane · Transition time · Transport number

✉ V. M. Barragán
vmabarra@ucm.es

¹ Department of Structure of Matter, Thermal Physics and Electronics, Faculty of Physics, Complutense University of Madrid, 28040 Madrid, Spain

² PoreLab, Department of Chemistry, Norwegian University of Science and Technology, 7491 Trondheim, Norway

1 Introduction

Charge transport properties of ion-exchange membranes are important in numerous applications, such as electrodialysis and reverse electrodialysis [1, 2]. Ion-exchange membranes are polymeric membranes that contain fixed charges in the polymer matrix. These allow passage of oppositely charged ions and obstruct ions of the same charge. Ideally, the charge transport number is unity. There are two main types of ion-exchange membranes, anion- and cation-exchange membranes, with positive and negative fixed charges, respectively. The efficiency of technologies mentioned rely largely on how well the ion-exchange membranes can exclude co-ions while simultaneously allowing transport of counter-ions. This ability is a fundamental property, often described as the membrane permselectivity. By permselectivity of an ion-exchange membrane we understand the transport number of the counter-ion involved in the process. As mentioned already, the transport number of the counter-ion of an ideal membrane is unity. This is thus the maximum attainable value for the membrane permselectivity [1, 3, 4].

Different methods have been used to determine the transference coefficient of a salt in a membrane. One of the methods often used is the electromotive method. In this method, there is a gradient in chemical potentials of salt and of water across the membrane. Both components contribute to the electromotive force of the cell (*emf*) [5]. If Ag|AgCl chloride reversible electrodes immersed in two 1:1 chloride solutions are used, the transport number of the salt is equal to the transport number of the cation in the membrane, \bar{t}_+ . The *emf* of whole cell can be expressed as [3, 5–7]:

$$\Delta\phi = -\frac{2RT}{F}\bar{t}_{\text{app}} \ln \frac{a_2}{a_1} \quad (1)$$

where a_1 and a_2 are the electrolyte activities at both sides of the membrane, and the relation $a_+a_- = a^2$ has been used [1, 7]. R and F are, respectively, the Gas and Faraday constants, T is the absolute temperature, and \bar{t}_{app} is the apparent transport number, which is related with the true cation transport by the expression [5, 6]:

$$\bar{t}_{\text{app}} = \bar{t}_+ - t_w M_s m_s \quad (2)$$

where M_s and m_s are, respectively, the molar mass and molality of the salt, and t_w is the transference number of water [5]. The *apparent* transport number, found in this method [8–11], refers to a concentration difference of the salt, masking the precise value of \bar{t}_+ . Other methods for direct determination of the ionic transport number are therefore of interest.

A potential method for direct determination of membrane permselectivity is chronopotentiometry [9, 12–14]. In this case, the concentration is the same on both sides of the membrane, and we can directly link the measurement to one concentration. However, when an electric current, I , is passing the ion-exchange membrane, concentration polarization may occur. A diffuse ion boundary layer will then form adjacent to the membrane. Theoretically, the electric current will reach a limiting value when the electrolyte concentration approaches zero near the membrane. Peers' equation, derived in 1956 [15], allows us to estimate the value of the limiting current

density, i_L , if we know the solute concentration, c_0 , the diffusion coefficient of solute in water, D , the boundary layer thickness, δ , the counter-ion transport number in the membrane, \bar{t}_i and its corresponding value in the solution, t_i :

$$i_L = \frac{DFc_0}{\delta(\bar{t}_i - t_i)} \quad (3)$$

The counter-ion transport number, which appears in Peers' equation, is the fraction of the electric current carried by migration of the ion in the electric field, in the absence of concentration differences or convective flow. The observed limiting current might in some cases exceed the value given by the Peers equation, however. The presence of convection will reduce the concentration polarization. Alternatively, conditions may lead to water splitting [16, 17].

The presence of electroconvection [18, 19] is an advantage in practice, as it helps avoid concentration polarization. This will allow reduction in expensive membrane area, meaning cost reduction. Water dissociation, however, may lead to an unwanted decrease of the current efficiency, meaning unwanted changes in the solution's pH [17, 20, 21]. Knowledge about the onset of the overlimiting behavior in ion-exchange membranes is thus important. Membrane bulk and surface heterogeneity affect membrane properties and consequently their performance in various processes. At a small enough scale, of micro- or nanometers, also homogeneous membranes appear heterogeneous, due to the existence of hydrophobic and hydrophilic parts in their structure.

In chronopotentiometry, the electric potential is measured in response to an imposed current. The method allows us to correlate significant transient states with the measured electric potential [22]. The method has been widely used for electrochemical characterization of ion-exchange membranes [22–36]. The transition time is the time at which the concentration of ions at the interface/membrane surface reaches zero value. For currents that exceed the limiting value, the transition time, τ_{Sand} , can be calculated by Sand's equation:

$$\tau_{\text{Sand}} = \frac{\pi D}{4} \left(\frac{c_0 z_i F}{\bar{t}_i - t_i} \right)^2 \frac{1}{j^2} \quad (4)$$

Here z_i is the charge number of counter-ion in the bulk electrolyte solution, and j is the membrane active surface average current density. Sand's equation can in principle be used to find ionic transport numbers in homogeneous permselective membranes, when all other variables are known, for the diffusion layer of finite thickness, and for current densities higher than a certain limiting value. The equation applies to transition times smaller than a certain value t^* , which can be estimated, from diffusion layer thickness as [10]:

$$t^* = \delta^2 / 2D \quad (5)$$

When $\tau_{\text{Sand}} < t^*$, a linear relation can be expected from Eq. 4, between transition time and the square of the inverse current density. The transition time is characteristic for the ion in question. Similar to Eq. 3, \bar{t}_i is the true transport number in the membrane

in the absence of water transport. The Sand Equation is often used to study the over-limiting ion transport mechanisms with the transport number as a known parameter. However, Eq. 4 would also allow us to determine the counter-ion transport number from experimental determination of transition times. Moreover, since in chronopotentiometry measurements, both cell compartments are filled with the same salt solution with the same concentration therefore, osmotic water transport does not contribute to the observed transport number, making the technique more precise [9, 11–13, 37–41].

The present work is motivated by the wish to find a better alternative to the *emf* method. To this purpose, we compare the results obtained by both methods, chronopotentiometry and electromotive force, as a function of the electrolyte concentration and use them to characterize the selective character of the ion-exchange membrane.

2 Experimental Section

2.1 Materials

Two commercial ion-exchange membranes manufactured by Fuma-Tech GmbH (Germany) were used in this work, one cationic and one anionic. Both are homogeneous and reinforced membranes with a PEEK polymer matrix. Fumasep® FKS–PET-75 (FKS) is a standard grade cation-exchange membrane for electrodialysis and reverse electrodialysis with an ion-exchange capacity of $0.8 \text{ meq}\cdot\text{g}^{-1}$ and a stated 98% selectivity. Fumasep® FAD–PET-75 anion-exchange membrane (FAD) is a special grade anion-exchange membrane with excellent properties regarding proton and anion transport as well as high efficiency with respect to metal ion rejection. Its ion-exchange capacity is $1.5 \text{ meq}\cdot\text{g}^{-1}$, with stated selectivity > 85%.

Aqueous solutions of sodium chloride of five different concentrations in the $1\text{--}100 \text{ mol}\cdot\text{m}^{-3}$ interval were used as electrolyte. This concentration interval was selected because water transport and polarization effects have high influence at low concentration. Pure pro-analysis grade chemical NaCl (Merck) and distilled pure water were used. The exact concentration of the electrolyte was determined measuring the electric conductivity of the prepared solution with a JENCO Model 1671 conductivity meter was used (See Table 3 in Appendix). The accuracy of the measurement was 1 and $10 \text{ }\mu\text{S}\cdot\text{cm}^{-1}$, in the low and high electrolyte concentration intervals, respectively. Prior to each experiment, the membrane to be used was immersed for a minimum of 24 h in the solution in order to achieve equilibrium.

2.2 Methods

2.2.1 Chronopotentiometry

The device used for chronopotentiometric and voltage-current curve experiments was similar to the one used in a previous work [31]. The effective area of the membrane was $2.27 \times 10^{-4} \text{ m}^2$. Chloride-reversible $\text{Ag(s)}|\text{AgCl(s)}$ -electrodes were

prepared with the method described in detailed elsewhere [42]. All experiments were carried out under isothermal conditions (25.0 °C). The temperature was constant within ± 0.1 °C. The measurements were carried out in absence of stirring (natural convection).

When the membrane system had been stabilized at the selected temperature, a constant electric current was made to pass through the membrane system over 300 s, and the voltage difference was recorded *vs* time. We started with a value slightly larger than the corresponding limiting current value. After 300 s, the electric current was interrupted, and values of the electric voltage were recorded during another period of 300 s. At the end of this period, the polarity was switched, and the whole experimental procedure was repeated under the same experimental conditions. This was done to maintain the chloride layers on the electrodes. The two polarity settings were labeled Case I (the original one) and case II (opposite polarity). The process was carried out, increasing gradually the values of the electric current.

To obtain the voltage–current curves in Case I, an electric current was applied, and the electric potential difference drop was recorded when state-steady was reached. The applied electric current was gradually increased, recording the stationary voltage in each case. The same procedure was repeated with opposite polarity (case II).

2.2.2 Electromotive Force

The device used for electromotive force experiments was similar to the one used in a previous work [43]. The cell consisted of two equal cylindrical glass chambers of a volume approximately 2×10^{-4} m³. A piece of Fumasep membrane with an effective 0.79×10^{-4} m² was placed vertically between the two chambers by means of two PVC disks fitting into each other. The system was placed in a water bath at a constant temperature $25.1 \text{ }^{\circ}\text{C} \pm 0.1 \text{ }^{\circ}\text{C}$ by means of a thermostat. A NaCl solution of $1 \text{ mol}\cdot\text{m}^{-3}$ (c_1) with a volume 1.7×10^{-4} m³ was introduced in one chamber. In the other chamber, the same volume of a NaCl solution of variable concentration $1\text{--}200 \text{ mol}\cdot\text{m}^{-3}$ (c_2) was introduced. The potential difference between two sides of the membrane was measured with Ag|AgCl reversible reference electrodes connected to a digital Keithley 195 System DMM, grounding the electrode corresponding to the chamber with lower concentration. The electrodes were prepared with the method describe in [42].

The determination of the electromotive force was carried out in the experimental device previously described. Prior to each experiment the membrane to be used was immersed a minimum of 24 h in the solution of lower concentration ($c_1 = 1 \text{ mol}\cdot\text{m}^{-3}$). Once the membrane was positioned in the cell, both chambers were filled with the solution of lower concentration. When the system was stabilized at the selective temperature and stirring rate, the electrodes were connected to the multimeter. In this situation the potential difference between two electrodes would be zero, however there can be seen a small bias, a potential difference that must be used to correct the measurements. A bias potential can be explained by small differences in the electrodes. Next, the concentration of solution in one chamber was kept constant (c_1), while it was changed in the other chamber from c_1 to c_2 , by adding a

certain volume of standard solution. The values of c_2 were changed in intervals of $1\text{--}200\text{ mol}\cdot\text{m}^{-3}$. After changing c_2 , the measured potential difference was stabilized in a few minutes. The values of the potential difference were recorded as a function of the higher concentration c_2 . The whole experimental process was carried out for the cation- as well as the anion-exchange membrane. In order to study if there were differences between new and used membrane samples, or in a membrane pack consisting in seven membranes samples placed together, the process was repeated with these three kind of membrane arrangements.

3 Results and Discussion

3.1 Voltage-Current Curves: Determination of the Limiting Current Value for the Membrane System

Voltage–current curves were similar for all the membrane systems. Figure 1 shows, as an example, the voltage–current density curve corresponding to FAD anion-exchange membrane at concentration C3. Cases I and II correspond to the different electrodes polarities.

From the voltage–current curves, the limiting current value was determined for all membrane system, using the Cowan diagram method, as it is shown in Fig. 1. The Cowan plot can be used to determine the value of the limiting current within

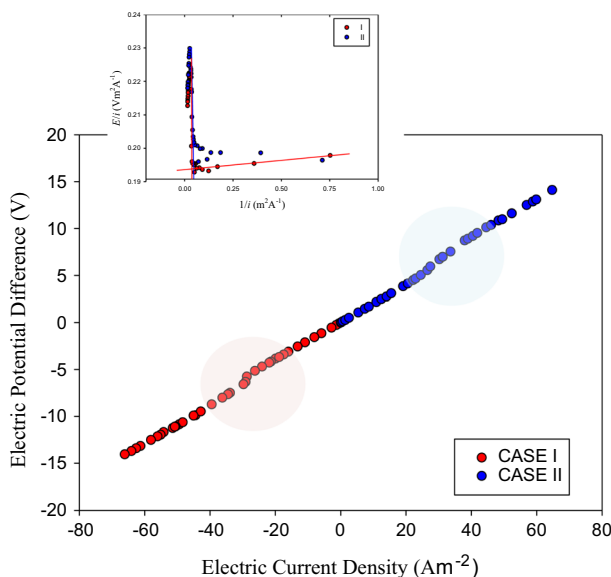


Fig. 1 Voltage–current density curves and corresponding Cowan diagrams. The data correspond to Fumasep FAD anion-exchange membrane at concentration C3 ($9.64\text{ mol}\cdot\text{m}^{-3}$). Cases I and II correspond to different electrodes polarities

1% when the plateau of the polarization curve is defined [44]. Results are shown in Table 1.

The values obtained agreed with values found in the literature for this kind of membranes using similar methods [20, 25, 45, 46]. For both membranes, the limiting current value increased with increasing electrolyte concentration, as can be expected [45, 46]. As the same electrolyte concentration, I_L values were higher for the anion membrane. This result is expected from Peers' equation taking into account that t_{Cl^-} is greater than t_{Na^+} in an aqueous solution, and given that we expect a transport number close to unity from the stated membrane selectivity. A small systematic difference in the limiting current densities was observed between the values obtained in Cases I and II. This difference was observed for all applied currents, and it increased by increasing the current, and more so for the anion than the cation-selective membrane. Case II results (from the second measurement) are systematically higher than Case I results. This difference could be explained by some conditioning taking place in the membranes in the first round of measurements or by the existence of an asymmetric membrane structure due to reinforcement [47]. But possible water splitting effects occurring during measurement in Case A could be also considered. Further work would be necessary to clarify this result.

3.2 Voltage–Time Curves: Determination of the Transition Time

Chronopotentiometric curves were obtained for all membrane systems using an applied electric current in overlimiting range $I > I_L$, cf. Table 1. For the Fumasep FKS cation-exchange membrane, an electric current density was applied varying in the intervals 0.29–0.80 mA·cm⁻², 0.78–1.49 mA·cm⁻², 2.02–2.91 mA·cm⁻², 11.8–19.1 mA·cm⁻², and 29.1–38.4 mA·cm⁻². For the Fumasep FAD anion-exchange membrane, the electric current varied in the intervals 0.630–1.21 mA·cm⁻², 1.54–2.93 mA·cm⁻², 2.91–4.48 mA·cm⁻², 16.3–31.8 mA·cm⁻², and 36.8–50.01 mA·cm⁻². The salt solutions were denoted C1, C2, C3, C4 and C5, respectively, varying from 1 mol·m⁻³ to 100 mol·m⁻³.

Table 1 Limiting current values, I_L , for Fumasep membranes in contact with solutions of NaCl of concentration c

Elec- trolyte sample	c (mol m ⁻³)	Fumasep FKS cation membrane		Fumasep FAD anion membrane	
		$I_L(10^{-3}A)$		$I_L(10^{-3}A)$	
		CASE I	CASE II	CASE I	CASE II
C1	1.01	0.14	0.18	0.30	0.31
C2	4.84	0.55	0.59	0.95	1.1
C3	9.64	1.23	1.49	1.90	2.2
C4	48.7	7.70	8.19	12.1	12.9
C5	99.8	16.6	17.5	29.7	32.7

Cases I and II refer to opposite polarities

The obtained chronopotentiograms were similar for all membrane systems, showing the typical shape for ion exchange membrane in binary solutions [22, 31, 36]. Figure 2 shows example curves, obtained for both membranes at concentration C3.

The moment the constant current was applied, there was an instantaneous rise in the electric voltage difference, corresponding to the ohmic voltage drop of the membrane-solution system. Afterwards, the voltage drop was almost constant with time, until the current was switched off, and a drop was observed within a second. However, when we applied a current above a certain value, the initial voltage continued to increase in time during the application. When the current density reached a characteristic value (j_L), a strong increase in voltage drop was registered.

The curves in Fig. 2 consist of two parts, a positive and a negative one, which correspond to the different electrodes polarities, Cases I and II, the purpose of which is to prevent electrode wear.

The sudden jump in electric potential difference across the membrane is due to the depletion of counter-ions at one of the membrane interfaces, and to the difference in transport number values between aqueous solution and the membrane. The limiting current defines the transition behavior and the range of currents where concentration polarization is intense and the supply of ions to the membrane surface is limited by diffusion. The time corresponding to the inflection point of voltage as a function of time is named the transition time, τ .

The transition time τ was estimated from the chronopotentiometric curve, the E - t derivative, as suggested in several references [46, 48–50]. This time corresponds to the maximum point of the derivative of the curve, and it has been determined calculating the time corresponding to the maximum value of the slope of the curve. It would represent the time at which the salt concentration at the membrane surface approaches zero. From this point, the flux of ions is maintained by

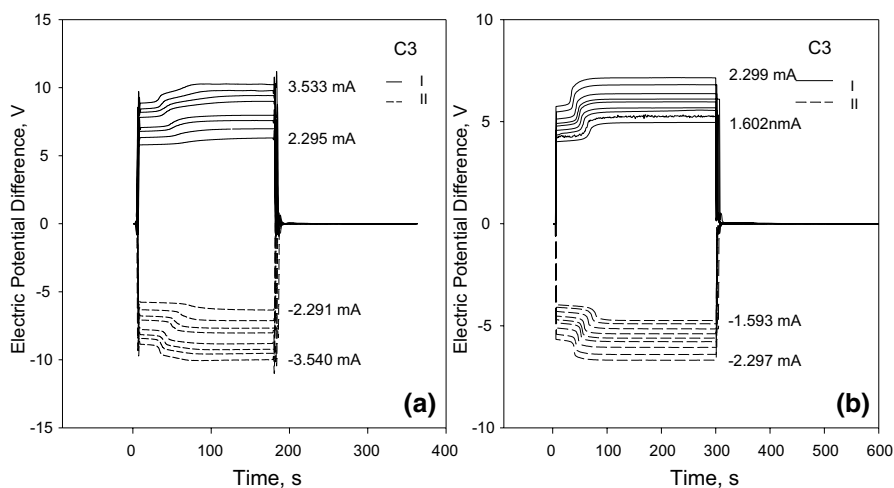


Fig. 2 Voltage–time curves at different applied electric currents for concentration C3 (9.64 mol·m⁻³) for the two investigated membranes. (a) Fumasep FAD-PET-75 anion-exchange membrane. (b) Fumasep FKS-PET-75 cation-exchange membrane. Cases I and II correspond to different electrodes polarities

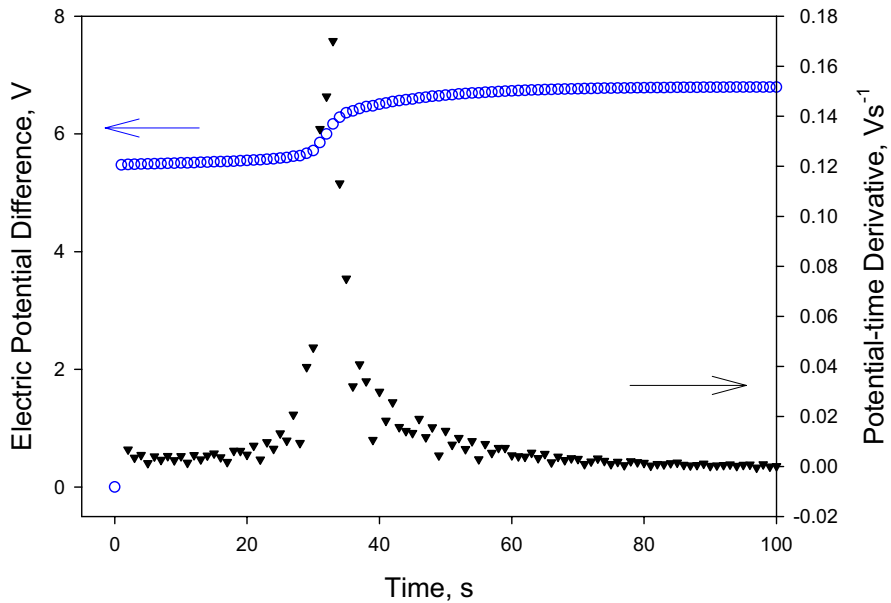


Fig. 3 Electric potential difference and potential-time derivative versus time curves for one of the studied cases. The data correspond to FKS membrane with $9.64 \text{ mol}\cdot\text{m}^{-3}$ and 2.30 mA (CASE I)

electro-convective fluxes in the case that electro-convection is the dominant mechanism of mass transfer in the overlimiting regime. Figure 3 presents an example of potential-time derivative versus time curve for one of the studied cases. The data correspond to membrane FKS and $9.64 \text{ mol}\cdot\text{m}^{-3}$ concentration. The behavior was similar to that of the anion membrane, and the maximum moved to the left when the current increased.

We calculated the Sand transition time for ideal membranes in the same conditions. For an ideal selective membrane, the Sand equation can be used to obtain the transition time in the membrane system if the appropriate solution properties are known. Comparing experimental results with numerical solutions, Valença [51] showed Sand's equation matches if $I > 1.2I_L$. An usual valid criterion is to apply electric currents higher than $1.5I_L$ to assure the validity of Sand's equation [30, 52]. Butylskii et al. [49] showed the inaccuracy does not exceed 0.3% in applying the Sand equation for $1.9I_L$ to estimate the transition time.

According to the Sand equation, under appropriate conditions, a linear relation should be observed between transition time τ and the inverse square of the current density. Figure 4 presents the obtained experimental transition times as a function of j^{-2} for all the membrane systems in Cases I and II, together with the value obtained from the Sand equation assuming ideal membranes. The values of concentration, diffusion coefficient and transport number in free solution are shown in Appendix (Table 3). To neglect the concentration dependence of the diffusion coefficient on the electrolyte concentration can lead to an incorrect estimate of the transition time [46, 53]. A linear behavior with j^{-2} is indeed observed after a given value of the

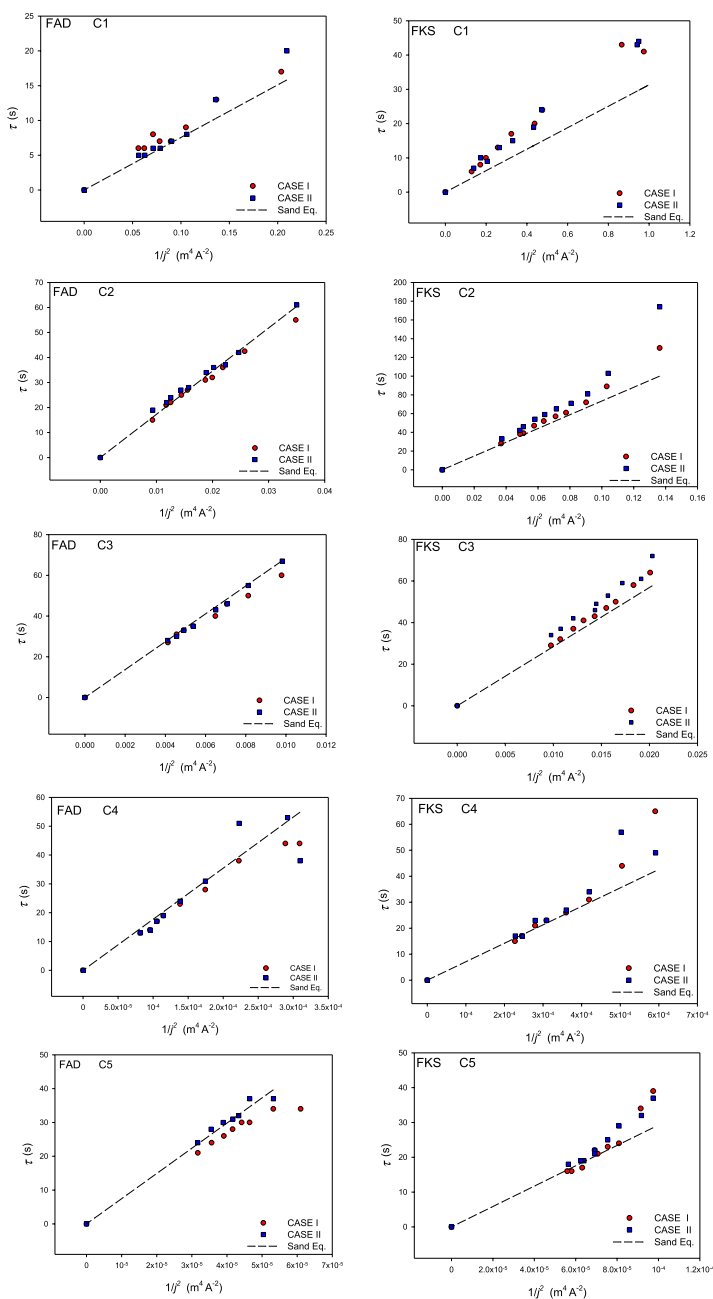


Fig. 4 Transition time versus inverse square of the electric current density. (a–e) Fumasep FKS-PET-75 cation-exchange membrane; (f–k) Fumasep FAD-PET-75 anion-exchange membrane. Dashed lines correspond to Sand transition times estimated from Sand equation for an ideal ion-exchange membrane with a counter-ion transport number equal to unity

applied current density. As can be observed, transition times (Cases I and II) are close to the transition times estimated from S and equation, especially for the anion-exchange membrane. This indicates that transition times τ may indeed be due to a difference in ion transport numbers between the solution phase and the membrane, leading to changing concentrations at the membrane surface and developing concentration polarization.

If convective electrolyte transport is not taken into account, an essential deviation between theoretical and experimental values of τ can occur under certain conditions. The observed deviation was higher for cation membranes in combination with small electrolyte concentrations. This cannot be explained by reduced membrane selectivity. A reduced selectivity or a smaller counter-ion transport number occur mainly at high concentrations [5, 54]. With the same chemical potential of water on the two sides of the membrane, there is also no contribution from osmosis, but well of electro-osmotic water transport. This is not included in the Sand equation. Normally, the ion transport number goes down when the electrolyte concentration increases [5, 54]. We are left to conclude that the conditions in the boundary layers can change significantly when the electrolyte concentration decreases, reflected also in an increasing uncertainty in the results.

The results seem to indicate that the interval of validity for the Sand equation depends on the electrolyte concentration. For the lowest concentration, a linear behavior is observed at current densities higher than $2I_L$, in agreement with [49]. However, for the highest concentration, a linear behavior is already observed at current densities higher than $1.5I_L$ for the cation membrane, and even at current slightly higher than the limiting value for the anion membrane.

3.3 Determination of Counter-Ion Transport Number in the Membrane Phase from Chronopotentiometry

From the linear fits to the Sand equation in the appropriate interval, we estimated the effective counter-ion transport number in the membrane from the slopes B of the curves, given by Eq. 6.

$$B = \frac{\pi D}{4} \left(\frac{c_0 z_i F}{\bar{t}_i - t_i} \right)^2 \quad (6)$$

To make sure that we applied Eq. 6 according to Eq. 4, we estimated the values of t^*_{ideal} considering an ideal permselective membrane with counter-transport number equal to unity. The thickness of the polarization layer for an ideal membrane was determined from Peers equation [55]. As the counter-transport number for real membranes are always lower than unity, the polarization layer for real membranes under the same conditions will be thicker than for the ideal membrane, and thus, also the value of t^* will be higher than the corresponding t^*_{ideal} . In all cases, we checked that the linear behavior in Fig. 4 appeared for times lower than the corresponding estimated t^*_{ideal} value and only these values were considered in the fit of experimental values to Eq. 6. Table 2 shows the values obtained for counter-ion transport numbers for both membranes at

Table 2 Parameter B and counter-ion transport numbers in the membrane in Cases I and II for the different studied membrane systems

c (mol m ⁻³)	FUMASEP FKS cation-exchange membrane			
	B_I (A ² s m ⁻⁴)	\bar{t}_{+I}	B_{II} (A ² s m ⁻⁴)	\bar{t}_{+II}
1.01	50 ± 4	0.884 ± 0.037	42 ± 1	0.928 ± 0.013
4.84	(81 ± 2) × 10	0.969 ± 0.015	(90 ± 1) × 10	0.939 ± 0.008
9.64	(30.2 ± 0.3) × 10 ²	0.983 ± 0.005	(34.8 ± 0.6) × 10 ²	0.942 ± 0.009
48.7	(74 ± 2) × 10 ³	0.985 ± 0.016	(82 ± 4) × 10 ³	0.952 ± 0.025
99.8	(30.1 ± 0.8) × 10 ⁴	0.992 ± 0.016	(32 ± 1) × 10 ⁴	0.975 ± 0.024
c (mol m ⁻³)	FUMASEP FAD anion-exchange membrane			
	B_I (A ² s m ⁻⁴)	\bar{t}_{-I}	B_{II} (A ² s m ⁻⁴)	\bar{t}_{-II}
1.01	85 ± 5	0.979 ± 0.022	82 ± 4	0.984 ± 0.021
4.84	(16.5 ± 0.4) × 10 ²	1.009 ± 0.009	(17.9 ± 0.4) × 10 ²	0.994 ± 0.009
9.64	(6.5 ± 0.1) × 10 ³	1.010 ± 0.007	(6.8 ± 0.1) × 10 ³	1.001 ± 0.006
48.7	(17.1 ± 0.6) × 10 ⁴	1.008 ± 0.013	(18 ± 1) × 10 ⁴	1.003 ± 0.025
99.8	(67 ± 2) × 10 ⁴	1.020 ± 0.013	(79 ± 2) × 10 ⁴	0.990 ± 0.008

the different electrolyte concentrations, together with the corresponding parameters B obtained from the fits. As can be observed, values close to unity were obtained in general as expected for highly selective membranes. In agreement with the results obtained for the limiting current values, slightly lower values were found for counter-transport numbers in Case II, although the difference is within experimental error.

A slight increase in the transport number was observed with increasing concentration, mainly for cation-exchange membranes. For the anion membrane, the differences are not systematic, they are within the experimental error. As it was previously commented, this trend with electrolyte concentration could be due to changes in the boundary layer. Zlotorowicz et al. [5], using similar FUMASEP membranes and the *emf* method, found a Na⁺ transport number of 0.93 and a chloride transport number of 0.998, in the cation- and anion membranes, respectively, for salt concentrations in the interval ~0.1–0.6 mol·kg. Under ideal conditions, the water transference coefficients for the membranes were 8 and 6, respectively, indicating that electroosmosis may play a role. Here we determine the transport number of the ion directly. The results agreed better for high NaCl concentrations [5]. A difference between the present and earlier result for Na⁺ in the membrane is expected, but cannot be related to a realistic number for water transference coefficient. While both methods seem to have high precision, there are uncertainties involved in the *emf* method related to the reference to the mean concentration, and in the chronopotentiometric method related to properties of the boundary layer next to the membrane. In this context it is valuable to have two independent methods.

We have found that chronopotentiometry can be used to find membrane ion transport numbers precisely and directly connected to an electrolyte concentration, without contributions from osmosis. But polarized layers are formed at both sides of a membrane, and electroosmosis may play a role also here. This would be relatively more significant at low concentrations.

3.4 Determination of the Mean Cation Transport Number in the Membrane Phase from Electromotive Force

Figure 5 shows the electromotive force measured as a function of the concentration of the concentrated solution c_2 in the concentration intervals 1–200 mol·m⁻³. The measurements were carried out with new and used membrane samples and also

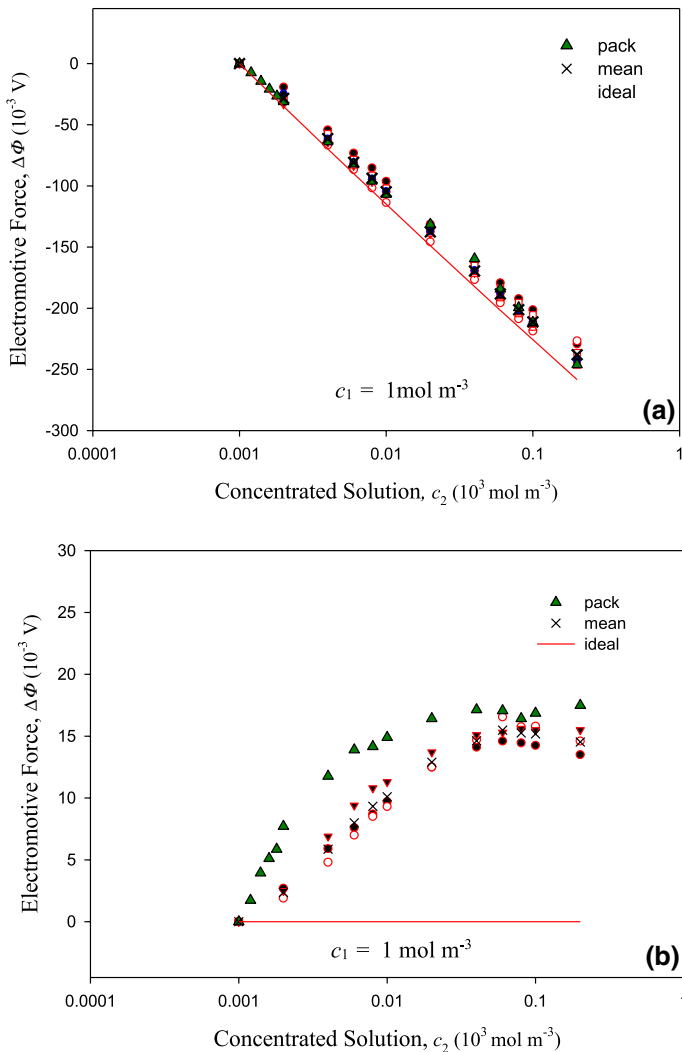


Fig. 5 Electromotive force versus concentration c_2 . (a) Fumasep cation-exchange membrane. (b) Fumasep anion-exchange membrane. Red (open circles) symbols correspond to measurements carried out with new membrane samples; blue (filled) symbols correspond to measurements carried out with used membrane samples; green (triangles) symbols correspond to the measurements carried out with a membrane pack. From the electromotive force values and using Eq. 1, apparent cation transport number in the membrane phase can be determined (Color figure online)

with a pack of seven membranes placed together. The purpose of using a pack of membranes was to minimize the salt diffusion as well as the osmotic water transfer through the membrane to avoid the change of the electrolytic concentration at both sides of the membrane.

As it can be observed in Fig. 5, no significant differences were observed between the values obtained using one sample (mean value of values obtained with new membranes) or the membrane pack (mean value of values obtained with pack of new membranes). The observed differences were a few millivolts. This is comforting as it indicates that diffusion has a negligible or small role. When membranes were reused, slightly lower values were obtained for both cation and anion membrane, although visually the difference is higher for anion membrane due to the difference of scale in two figures. In order to minimize ion diffusion and osmotic water transfer through the membrane, a mean value of the results obtained with the pack were used in the determination of the apparent transport numbers. With the electrode connected to the lower concentration chamber grounded, the measured electromotive force was negative for cation-exchange membrane, as was expected. For the anion-exchange membrane, a lower negative value would also be expected. However, positive values were observed, indicating that other effects, in addition to the membrane potential, contribute to the measured electromotive force.

The values obtained for the apparent cation transport number, according to Eq. 1 are presented in Fig. 6.

The transport number obtained by this method is only a mean apparent transport number in the interval of concentration c_1 – c_2 . For this reason, they could be considered as the apparent transport number at the mean concentration of the two electrolytes in contact at both sides of the membrane. Figure 6 also presents the mean value of the cation transport number obtained in cases I and II by chronopotentiometry. As can be observed, the main differences between the results obtained by both methods are presented at low concentrations. Higher values were obtained using chronopotentiometry, decreasing the observed difference with concentration increasing. From the transport numbers obtained with chronopotentiometry method, it can be supposed that the transport number has not a great dependence on the electrolyte concentration in the investigated interval, with the exception of the lower concentrations. It's known that water transport decreases with the electrolyte concentration and that the influence is higher at low concentration values [56]. Moreover, in spite of the solutions being strongly stirred, the polarization layers cannot be completely eliminated and it is known that concentration polarization effects are higher at low electrolyte concentration [57]. This could explain the trend in the cation transport number observed in Fig. 6. When the solution concentration increases, both polarization effects and water contribution decrease, and the ion transport numbers tend to unity for both membranes. The obtained results seem to indicate that these effects would have largest influence in the electromotive force method.

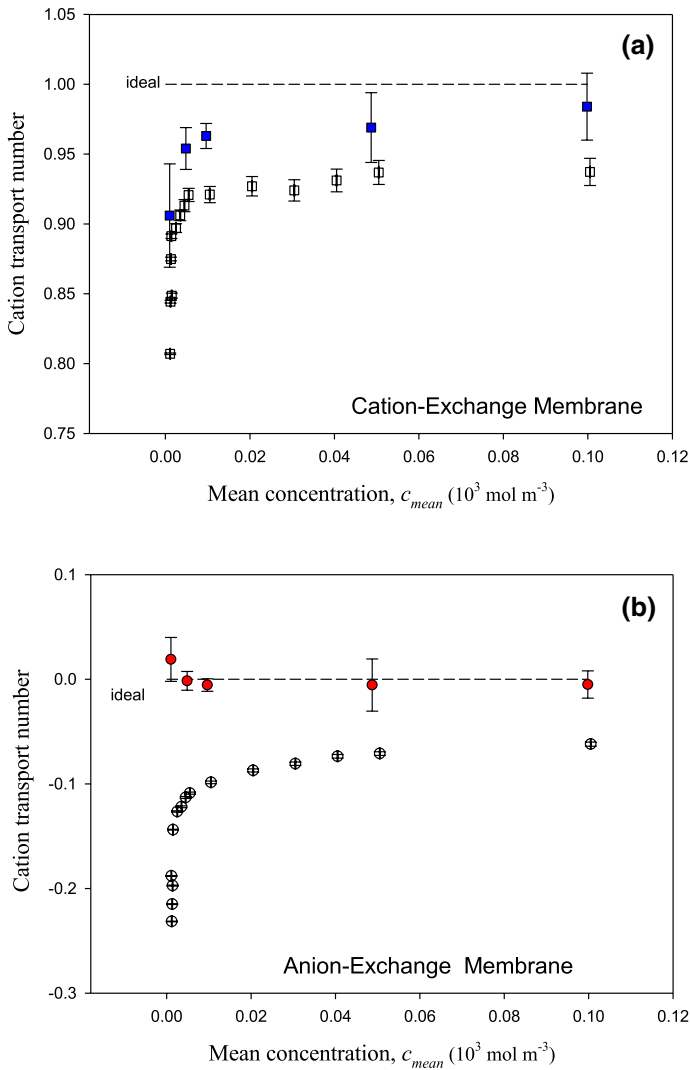


Fig. 6 Sodium transport number in the membrane phase as a function of the mean electrolyte concentration estimated from chronopotentiometry (full symbols) and from *emf* (empty symbol). (a) FKS cation-exchange membrane. (b) FAD anion-exchange membrane

4 Conclusions

We have reported cation transport numbers for the anion- and cation exchange membranes from FUMASEP in NaCl solutions determined by chronopotentiometry and electromotive force methods. Membranes submerged in solutions of NaCl varying

Table 3 Concentration, electric conductivity, diffusion coefficient and transport number of ion sodium in free solution, for the used electrolytes at 25°C

Electrolyte	c (mol·m ⁻³)	σ (10 ⁻³ S·cm ⁻¹)	D (10 ⁻⁹ m ² ·s ⁻¹)	$t_{\text{Na}+}$
C1	1.01	0.126	1.584	0.3954
C2	4.84	0.581	1.561	0.3935
C3	9.64	1.14	1.547	0.3919
C4	48.7	5.42	1.529	0.3891
C5	99.8	10.65	1.518	0.3852

between 1 mol·m⁻³ and 100 mol·m⁻³ were found to be close ideal in most of the cases.

The cation transport number estimated by the electromotive force method was systematically lower than the number obtained from chronopotentiometry, probably due to larger concentration polarization at low electrolyte concentration. We conclude that chronopotentiometry is a relatively more rapid and precise technique for ion transport number determination at electrolyte concentrations for which membranes maintain a good selectivity and that it is lower affected than electromotive method by water transfer effects at low electrolyte concentrations.

Appendix

The electric conductivity of the solutions used in the chronopotentiometry measurements was measured according to the method previously described. From the obtained values, the exact concentration of the prepared solutions can be determined from tabulated values of the electric conductivity σ (S·cm⁻¹) versus concentration c (mol·L⁻¹) for NaCl solutions at 25 °C [58, 59]. Known the true concentration of each electrolyte solution, the diffusion coefficient D and the transport number of ion sodium in free solution t_+ were estimated from tabulated data for the different electrolyte solutions [58, 59]. The results are showed in Table 3.

Acknowledgements Financial support from Banco de Santander and Universidad Complutense de Madrid under Project PR75/18-21589 is gratefully acknowledged. K.R.K. and S.K. are grateful to Research Council of Norway for project no 262644 PoreLab.

References

1. F.G. Helfferich, *Ion Exchange* (McGraw-Hill, New York, 1962)
2. T. Luo, S. Abdu, M. Wessling, Selectivity of ion exchange membranes: a review. *J. Membr. Sci.* **555**, 428 (2018)
3. H. Strathmann, *Ion-Exchange Membrane Separation Processes, Membrane Science and Technology Sciences*, vol. 9 (Elsevier, Amsterdam, 2004)
4. Y. Tanaka, *Ion-Exchange Membranes*, vol. 12, 2nd edn. (Elsevier Science, Amsterdam, 2015)
5. A. Zlotowicz, R.V. Strand, O.S. Burheim, O. Wilhelmsen, S. Kjelstrup, The permselective and water transference number of ion exchange membranes in reverse electrodialysis. *J. Membr. Sci.* **523**, 402 (2017)

6. N. Lakshminarayanaiah, *Transport Phenomena in Membranes* (Academic Press, New York, 1969)
7. G.M. Geise, H.J. Cassidy, D.R. Paul, B.E. Logan, M.A. Hickner, Specific ion effects on membrane potential and the permselectivity of ion exchange membranes. *Phys. Chem. Chem. Phys.* **16**, 21673 (2014)
8. C. Larchet, B. Auclair, V. Nikonenko, Approximate evaluation of water transport number in ion-exchange membranes. *Electrochim. Acta* **49**, 1711 (2004)
9. R.K. Nagarale, V.K. Shahi, S.K. Thampy, R. Rangarajan, Studies on electrochemical characterization of polycarbonate and polysulfone based heterogeneous cation-exchange membranes. *React. Funct. Polym.* **61**, 131 (2004)
10. R.H. Nagarale, G.S. Gohil, V.K. Shahi, Recent developments of ion-exchange membranes and electro-membrane processes. *Adv. Colloid Interface Sci.* **119**, 97 (2006)
11. G.S. Gohil, V.V. Binso, V.K. Shahi, Preparation and characterization of mono-valent in exchange polypyrrole composite ion-exchange membranes. *J. Membr. Sci.* **280**, 210 (2006)
12. A.A. Mansoor, M. Mustakeen, D. Nedela, Study the transport properties of anion and cation exchange membranes toward various ion using chronopotentiometry. *Iran J. Chem. Chem. Eng.* **36**, 81 (2017)
13. L. Marder, E.M. Ortega Navarro, V. Pérez-Herranz, A.M. Bernardes, J. Zoppas Ferreira, Evaluation of transition metal transport properties through a cation-exchange membrane by chronopotentiometry. *J. Membr. Sci.* **284**, 267 (2006)
14. V.K. Shashi, R. Prakash, G. Ramachandraiah, R. Rangaranjan, D. Vasudevan, Solution-membrane equilibrium at metal-deposited cation-exchange membranes: chronopotentiometric characterization of metal-modified membranes. *J. Colloid Interface Sci.* **216**, 179 (1999)
15. A.M. Peers, General discussion. *Discuss. Faraday Soc.* **21**, 124 (1956)
16. V.V. Nikonenko, A.V. Kovalenko, M.K. Urtenov, N.D. Pismenskaya, Desalination at overlimiting currents: State-of-the-art and perspectives. *Desalination* **324**, 85 (2014)
17. V.V. Nikonenko, N.D. Pismenskaya, E.I. Belova, P. Sistat, P. Huguet, G. Pourcelly, C. Larchet, Intensive current transfer in membrane systems: Modelling, mechanisms and application in electrodialysis. *Adv. Colloid Interface Sci.* **160**, 101 (2010)
18. E.I. Belova, G.Y. Lopatkova, N.D. Pismenskaya, V.V. Nikonenko, C. Larchet, G. Pourcelly, Effect of anion membrane surface properties on mechanisms of overlimiting mass transfer. *J. Phys. Chem. B* **110**, 13458 (2006)
19. F. Roghman, E. Evdochenko, F. Stockmeier, S. Schenider, A. Smaijili, R. Towari, A. Mikosh, E. Kataray, A. Kühne, A. Walther, A. Mani, M. Wessling, 2D patterned ion-exchange membranes induces electroconvection. *Adv. Mater. Interfaces* **61**, 801309 (2019)
20. V.I. Zabolotsky, V.V. Nikonenko, N.D. Pismenskaya, E.V. Laktionov, M.K. Urtenov, H. Strathmann, M. Wessling, G.H. Koops, Coupled transport phenomena in overlimiting current electrodialysis. *Sep. Purif. Technol.* **14**, 225 (1998)
21. Y. Tanaka, Water dissociation reaction generated in an ion exchange membrane. *J. Membr. Sci.* **350**, 347 (2010)
22. H. Strathmann, Chronopotentiometry for the advanced current-voltage characterization of bipolar membranes. *J. Electr. Chem.* **502**, 152 (2001)
23. M. Taky, G. Pourcelly, C. Gavach, A. Elmidaoui, Chronopotentiometric response of a cation exchange membrane in contact with chromium (III) solutions. *Desalination* **105**, 219 (1996)
24. J.H. Choi, S.-H. Moon, Pore size characterization of cation-exchange membranes by chronopotentiometry using homologous amine ions. *J. Membr. Sci.* **191**, 225 (2001)
25. R. Ibañez, D.F. Stamatis, M. Wessling, Role of membrane surface in concentration polarization at cation exchange membranes. *J. Membr. Sci.* **239**, 119 (2004)
26. N. Pismenskaia, P. Sistat, P. Huguet, V. Nikonenko, G. Pourcelly, Chronopotentiometry applied to the study of ion transfer through anion exchange membranes. *J. Membr. Sci.* **228**, 65 (2004)
27. T. Sata, *Ion Exchange Membranes: Preparation, Characterization, Modification and Application* (Royal Society of Chemistry, Cambridge, 2004)
28. P. Dugolecki, B. Anet, S.J. Metz, K. Nijmeijer, M. Wessling, Transport limitation in ion exchange membranes at low salt concentration. *J. Membr. Sci.* **346**, 163 (2010)
29. C. Larchet, S. Nouri, B. Auclair, L. Dammak, V. Nikonenko, Application of chronopotentiometry to determine the thickness of diffusion layer adjacent to an ion-exchange membrane under natural convection. *Adv. Colloid Interface Sci.* **139**, 45 (2008)

30. S.A. Mareev, V.S. Nichka, D.Y. Butylskii, M.K. Urtenov, N.D. Pismenskaya, P.Y. Apel, V.V. Nikonenko, Chronopotentiometric response of an electrically heterogeneous permselective surface: 3D modelling of transition time and experiment. *J. Phys. Chem. C* **120**, 13113 (2016)
31. Y. Freijanes, V.M. Barragán, S. Muñoz, Chronopotentiometric study of a Nafion membrane in presence of glucose. *J. Membr. Sci.* **510**, 79 (2016)
32. L. Vobecká, M. Svoboda, J. Benes, T. Bellon, Z. Slouka, Heterogeneity of heterogeneous ion-exchange membranes investigated by chronopotentiometry and X-ray computed microtomography. *J. Membr. Sci.* **559**, 127 (2018)
33. J.J. Krol, M. Wessling, H. Strathmann, Chronopotentiometry and overlimiting ion transport through monopolar ion exchange membranes. *J. Membr. Sci.* **162**, 155 (1999)
34. M.C.C. Martí-Calatayud, D.C.B. Buzzi, M. García-Gabaldón, A.M.M. Bernardes, J.A.S. Tenório, V. Pérez-Herranz, Ion transport through homogeneous and heterogeneous ion-exchange membranes in single salt and multicomponent electrolyte solutions. *J. Membr. Sci.* **466**, 45 (2014)
35. L. Marder, E.M. Oretaga Navarro, V.O. Pérez-Herranz, A.M. Bernardes, J.Z. Ferreira, Evaluation of transition metals transport properties through a cation-exchange membrane by chronopotentiometry. *J. Membr. Sci.* **284**, 267 (2006)
36. T. Scarazzato, Z. Panossian, M. García-Gabaldón, E.M. Ortega, J.A.S. Tenório, V. Pérez-Herranz, D.C.R. Spinosa, Evaluation of the transport properties of copper ions through a heterogeneous ion-exchange membrane in etidronic acid solutions by chronopotentiometry. *J. Membr. Sci.* **535**, 268 (2017)
37. P. Ray, V.K. Shahu, T.V. Pathak, G. Ramachandraiah, Transport phenomenon as a function of counter and co-ions in solution: chronopotentiometric behaviour of anion exchange membrane in different aqueous electrolyte solutions. *J. Membr. Sci.* **160**, 243 (1999)
38. S. Koter, C. Güler, I. Koter, Chronopotentiometric characterization of electrodialysis module. *Archit. Civ. Eng. Environ.* **3**, 129 (2016)
39. M.C. Martí-Calatayud, M. García-Gabaldón, V. Pérez-Herranz, E. Ortega, Determination of transport properties of Ni(II) through a Nafion cation-exchange membrane in chromic acid solutions. *J. Membr. Sci.* **379**, 449 (2011)
40. G. Vázquez-Rodríguez, L.M. Torres-Rodríguez, A. Montes-Rojas, Synthesis and characterization of commercial cation-exchange membranes modified electrochemically by polypyrrole: effect of synthesis conditions on the transport properties. *Desalination* **416**, 94 (2017)
41. S.A. Mareev, D.Y. Butylskii, A.V. Kovalenko, D.D. Pismenskaya, L. Dammak, C. Larchet, V.V. Nikonenko, Inclusion of the concentration dependence of the diffusion coefficient in the Sand equation. *Russ. J. Electrochem.* **52**, 996 (2016)
42. G.J. Janz, Silver-silver halide electrodes, in *Reference Electrodes*, ed. by D.J.G. Ives, G.J. Janz (Academic Press, London, 1961), p. 179
43. V.M. Barragán, C. Ruiz-Bauzá, Membrane potential and electrolyte permeation in a cation-exchange membrane. *J. Membr. Sci.* **154**, 261 (1999)
44. C. Ponce-de-León, C.T.J. Low, G. Kear, F.C. Walsh, Strategies for the determination of the convective-diffusion limiting current from steady linear sweep voltammetry. *J. Appl. Electrochem.* **37**, 1261 (2007)
45. V.M. Barragán, C. Ruizá, Current-voltage curves for ion-exchange membranes: a method for determining the limiting current density. *J. Colloid Interface Sci.* **205**, 365 (1998)
46. X.T. Le, T.H. Bui, P. Viel, T. Berthelot, S. Palcin, On the structure-properties relationship of the AMV anion exchange membrane. *J. Membr. Sci.* **340**, 133 (2009)
47. L. Gurreri, A. Filingeri, M. Ciofalo, A. Cipollina, M. Tedesco, A. Tamburini, G. Micale, Electrodialysis with a profile geometry on current phenomena. *Desalination* **506**, 115001 (2021)
48. S.A. Mareev, D.Y. Butylskii, N.D. Pismenskaya, V.V. Nikonenko, Chronopotentiometry of ion-exchange membranes in the overlimiting current range. Transition time for a finite-length diffusion layer: modelling and experiment. *J. Membr. Sci.* **500**, 171 (2016)
49. D.Y. Butylskii, S.A. Mareev, N.D. Pismenskaya, P.Y. Apel, O.A. Polezhaeva, Phenomenon of two transition times in chronopotentiometry of electrically inhomogeneous ion exchanges membranes. *Electrochim. Acta* **273**, 289 (2018)
50. S.A. Mareev, A.V. Nebavskiy, V.S. Nichka, M.K. Urtenov, The nature of two transition times on chronopotentiograms of heterogeneous ion exchange membranes: 2D modelling. *J. Membr. Sci.* **575**, 179 (2019)
51. J. C. Valença, Overlimiting current properties at ion exchange membranes, PhD Thesis Universiteit Twente, 2017

52. M. van Soestbergen, P.M. Biesheuvel, M.Z. Bazant, Diffuse-charge effects on the transient response of electrochemical cells. *Phys. Rev. E* **81**, 021503 (2010)
53. S.A. Mareev, D.Y. Butylskii, A.V. Kovalenko, A.V. Petukhova, N.D. Pismenskaya, Accounting for the concentration dependence of electrolyte diffusion coefficient in the Sand and the Peers equations. *Electrochim. Acta* **195**, 85 (2016)
54. S. Koter, Transport number of counterions in ion-exchange membranes. *Sep. Purif. Technol.* **22**, 643 (2001)
55. D.Y. Butylskii, E.D. Skolotneva, S.A. Mareev, A.D. Gorobchenko, M.K. Urtenov, Estimation of the equations for calculation of chronopotentiometric transition time in membrane systems. *Electrochim. Acta* **353**, 136595 (2020)
56. V.M. Barragán, C. Ruiz-Bauzá, J.I. Mengual, On current dependence of the electroosmotic in ion-exchange membranes. *J. Membr. Sci.* **95**, 1 (1994)
57. V.M. Barragán, C. Ruiz-Bauzá, J.I. Mengual, Effect of unstirred solution layers on electroosmotic permeability of cation-exchange membranes. *J. Colloid Interface Sci.* **168**, 458 (1994)
58. R.A. Robinson, R.H. Stokes, *Electrolyte Solutions* (Academic Press, New York, 1959)
59. V.M.M. Lobo, *Electrolyte Solutions: Literature Data on Thermodynamics and Transport Properties* (Coimbra Editora, Coimbra, 1975)

Publisher's Note Springer Nature remains neutral with regard to jurisdictional claims in published maps and institutional affiliations.